Fractal Analysis of Thin Films Surfaces: A Brief Overview

Fredrick M. Mwema, Esther T. Akinlabi and Oluseyi P. Oladijo

Abstract The concept of fractals has been widely accepted in various fields for studying natural or random phenomena. Most specifically, in surface engineering and thin films, fractal analysis is used to investigate the self-affine nature and scaling characteristics of surfaces to understand the physical processes of creating the surfaces. Various methods have been applied in the fractal analysis of thin films, some of which include autocorrelation, height-height correlation, power spectral density functions, triangulation, and box counting among others. From these methods, it is possible to compute the roughness characteristics such as roughness exponent, correlation length, fractal dimension, Hurst exponent, etc. Fractal dimension is the key parameter used to understand the roughness properties of the films. In this article, we have summarised some of the key results on the fractal analysis of thin films, and it has been noted that fractal characteristics depend on the thin films' deposition processes. The interrelationships among the fractal parameters and surface morphology of the films are unpredictable, and therefore fractal analysis should be undertaken for each new type of thin films.

Keywords Atomic force microscope · Autocorrelation · Fractals · Roughness · Self-affine · Thin films

F. M. Mwema (✉) · E. T. Akinlabi · O. P. Oladijo
Department of Mechanical Engineering Science, University of Johannesburg, Johannesburg 2006, South Africa
e-mail: fredrick.mwema@dkut.ac.ke

O. P. Oladijo
Department of Chemical, Materials and Metallurgical Engineering, Botswana University of Science and Technology, Private Bag 16, Palapye, Botswana

M. Awang et al. (eds.), *Advances in Material Sciences and Engineering*, Lecture Notes in Mechanical Engineering,
https://doi.org/10.1007/978-981-13-8297-0_28

1 Introduction

1.1 Background

The concept of fractals has been accepted to describe most natural systems and currently finding extensive application in the characterisation of surfaces [1, 2]. In most cases, random systems such as surface microscopy behave like fractals, i.e. their geometrical units resemble one another at all scales (at both low and high magnification similar features are identified) [3–5]. It, therefore, means that fractals are not sensitive to the scale of resolution and fractal analysis can be used to extract more information about a surface as compared to the conventional statistical methods [6]. The concept of fractals in thin film structures was clearly described, for the first time, in 1985 by Yehoda and Messier [7]. They argued that the presence of low-density regions (network of voids) of films microstructures was the reason for the fractal behaviour of thin films. In thin film surfaces, fractal dimension is used as an analytical index to measure how the morphological features vary on scaling [2]. The fractal analysis provides information on roughness exponent, correlation length, shift (or lattice size) and pseudo-topothesy besides the fractal dimension of thin films [8]. These parameters offer a detailed description of spatial patterning, segmentation, texture and lateral roughness of the surface morphology [9]. As such extensive literature exists on fractal analysis of surfaces of thin films [10–19] and several methods of fractal analysis, have been developed. The objective of this paper is to provide a very short overview of the most commonly used methods and summarize some of the published results of fractal analysis of thin films. The article may assist researchers expecting to use these methods in thin film imaging applications.

1.2 A Review of Common Fractal Analysis Methods

1.2.1 Autocorrelation Function

The autocorrelation function (ACF) shows the dependence of a signal on its own at different time shifts. In thin films, ACF describes the self-affine characteristics of surfaces and is used to derive fractal parameters such as roughness exponent, correlation length and fractal dimension (D) [12]. From various literatures [20, 21], the autocorrelation function (A(r)) along the direction of fast scan (x-direction) is expressed in terms of height function z(i, j) as follows.

$$A(r = ld) = \frac{1}{m(m-l)w^2} \sum_{j=1}^{m} \sum_{i=1}^{m-l} z(i+l, j) z(i, j) \tag{1}$$

where d is the horizontal distance between two adjacent image features and l is the preceding feature of the point (m) of interest.

1.2.2 Height-Height Correlation Function

Various researchers have used height-height correlation function (H(r)) to illustrate the self-affine and mounded characteristics of surfaces of thin films [1, 6, 12, 13]. Mathematically, one-dimensional H(r) of the m × m area of surface micrograph in the direction of the fast scan of the AFM probe is given as follows [22].

$$H(r = ld) = \frac{1}{m(m-l)} \sum_{j=1}^{m} \sum_{i=1}^{m-l} [z(i+l, j) - z(i, j)]^2 \tag{2}$$

A bi-logarithmic plot of H(r) versus r reveals two regimes as described by Yadav et al. [12] and it has been shown that the fractal dimension (D) is determined by fitting a power law within the linear region (small values of r) of the plot whereas roughness exponent, correlation lengths and Hurst exponents are determined by best-curve at the nonlinear region (large values of r). Detailed applications of H(r) are reported elsewhere [1, 12, 20].

1.2.3 Power Spectral Density Function

The power spectral density function uses a fast Fourier transform algorithm of the height functions (H_st) of the surface as shown in the logarithmic diagram in Fig. 1a. The fractal dimension is computed as a function of the average power (S) of the height spectra over the area under study and is determined as follows [23].

$$S = \frac{1}{l^2 N_j} \sum_{1}^{N_j} |H_{st}|^2 \tag{3}$$

where Nj is the number of points within the digital area whose linear size is defined by l. Within the highly correlated region (self-affine surfaces), S obeys the power law in the form $\boldsymbol{S} = \boldsymbol{k}_{\boldsymbol{j}}^{-\boldsymbol{\beta}-\mathbf{1}}$ where, kj is the radial spatial frequency and the slope of the curve in Fig. 1b is defined by β [24]. From this method, D can be determined as follows.

$$\boldsymbol{D} = \frac{\mathbf{7} - \boldsymbol{\beta}}{\mathbf{2}} \tag{4}$$

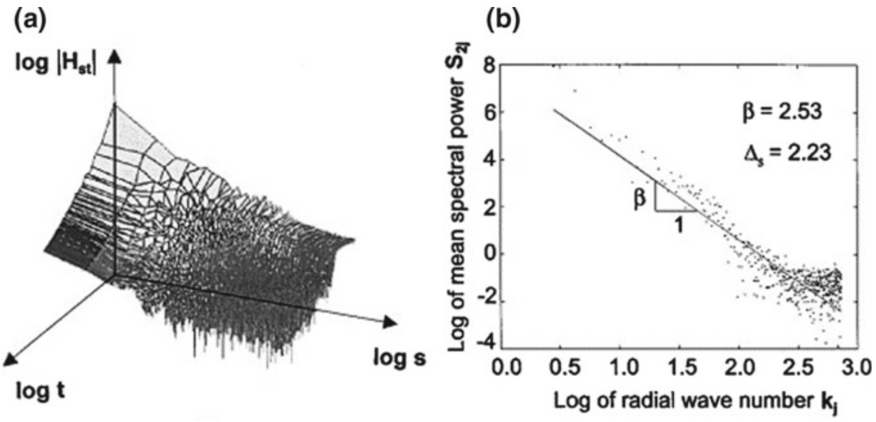

Fig. 1 Illustrating the spectral determination of the fractal dimension through (**a**) fast Fourier transform of surface and (**b**) the double log plot of power versus spatial frequency (adapted from Carpinteri et al. [23] with permission from Elsevier, copyright order number 501448072)

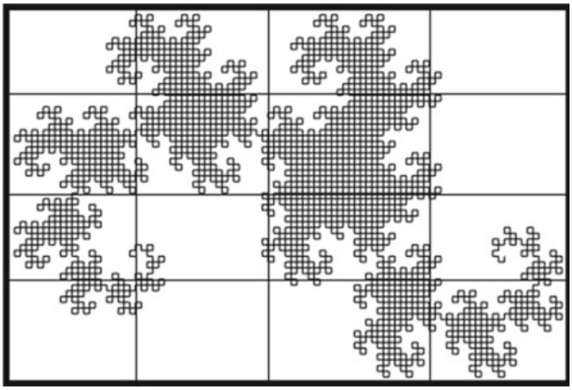

Fig. 2 Illustrating the box-counting method for dragon curve fractals. In this method, N is the number of the boxes and h is the length scale (size of each box)

1.2.4 Box-Counting Method

In this method, the fractal features are covered with a single box, which is subsequently divided into four quadrants. Each of the quadrants is further divided into four quadrants, and this is repeated in a loop until the minimum size of each box is equal to the resolution of the data [25, 26]. Then for each case, the number of boxes (N) covering the fractal features are counted, and its logarithm is plotted versus the size of boxes (h). The fractal dimension (D) is determined from the maximal slope coefficient of the double log plot defined as follows [25, 27, 28]. The method is illustrated in Fig. 2.

$$D = \lim_{h \to 0} -\frac{\log N(h)}{\log h} \quad (5)$$

1.2.5 Triangulation Method

The computation of D in triangulation method (as known as prism counting) is based on approximating the area of the surface using successive pyramids and computing their lateral regions as illustrated in Fig. 2 [23, 29]. The area under study is covered by a square patch, and then one pyramid on the four angles of the square is created (Fig. 3a). The square is further subdivided into four quadrants, and then on each quadrant, a pyramid is created so that a total of 8 pyramids are generated (Fig. 3b).

The procedure is repeated to generate 16 pyramids (Fig. 3c), 32 pyramids (Fig. 3d) and so forth until the base length of each pyramid (r) is equal to the resolution of the digital data of the image. The apparent area (A) of each prism is then computed for each r. The slope of the bi-logarithmic plot of r versus A is used to compute D as follows [23].

$$D = 2 - \lim_{r \to 0} - \frac{\log \mathrm{A}(r)}{log\, r} \tag{6}$$

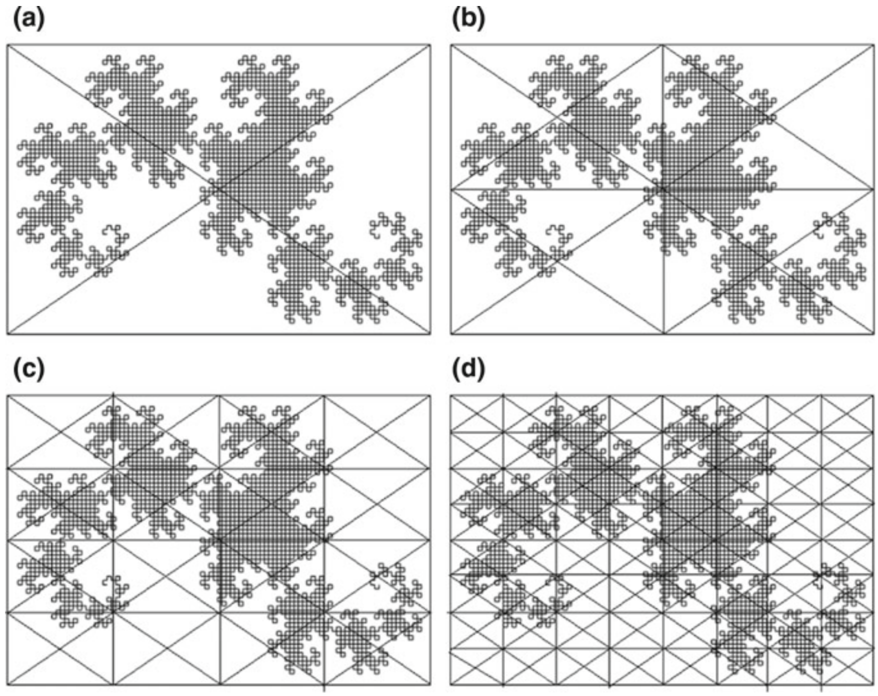

Fig. 3 Triangulation fractal dimension scheme of the dragon curve fractal. The **a**, **b**, **c**, **d** represents the repetitive steps followed in constructing the pyramids for each rectangular space occupied by the fractal features

2 Overview of Published Literature

There is considerable published literature on the fractal analysis of thin films. The general observation from literature is that fractal methods provide a detailed description of the microstructure and evolution of the physical structures during thin film deposition. Through, fractal methods, the evolution of surface complexity of structure with the deposition parameters has been detailed [1, 13, 17, 24, 30]. The fractal dimension has been shown to increase/decrease with the substrate temperature, power and films' thickness [1, 31, 32]. In a recent study, the effect of deposition time on the sputtering of Ti thin films on glass substrate was reported and shown that the fractal dimension increases with the deposition time [33]. Ţălu et al. [34] reported on the variation of fractal dimension of Ni–C prepared through the combination of radio frequency sputtering and plasma enhanced chemical vapor deposition (PEVD) techniques at varying times of 7, 10, 13 min on silicon and glass substrates. The highest fractal dimension was obtained at 10 min while the lowest obtained at 13 min of deposition. The fractal dimension has also been shown to decrease with increase in PEVD deposition pressure [35]. The power spectral density of 10 and 20 nm gold thin films has been reported [36]. The effect of annealing temperatures on the fractal properties of ITO thin films deposited by electron beam evaporation has been reported [37, 38]. Using height-height correlation method, Raoufi et al. [37] reported that fractal dimension of ITO films increases with the annealing temperature. Similar results were reported for the same films using power spectral density method [3]. In a similar study, Raoufi [38] reported that the lower annealing temperature, the slower the decrease of the fractal dimension. The fractal dimension of AlN epilayers sputtered on alumina was shown to increase with the substrate temperature [31]. The effect of deposition power and substrate temperature of Al thin films on steel substrates has been described by power spectral density function [24, 30]. The relationship between the statistical and fractal measurements of thin films has also been reported by various researchers [14, 24, 30, 39]. The general finding from these reports is that there is no direct relationship between root mean square and average roughness and fractal dimension.

Table 1 provides a summary of some of the fractal methods used in thin film analysis. The results of the correlation among the properties, deposition methods/parameters and fractal characteristics of the thin films are also included in Table 1.

3 Conclusions

Fractal techniques offer powerful tools for characterisation and segmentation of surface structures of thin films. The fractal dimension is the basic measure of irregularity and discontinuities of the surface properties. Various methods have been used for computation of fractal dimension of thin films some of which include, autocorrelation, height-height correlation functions, power spectrum and box counting methods.

Table 1 Selected published articles and key results on the fractal analysis of thin films

Author/year	Description of the publication	Fractal analysis method(s) used	Findings and inferences
Yadav et al. [12]/2014	Fractal characteristics of LiF thin films deposited through electron beam evaporation at 77, 300 and 500 K substrate temperatures were reported	Height-height autocorrelation	The lateral correlation lengths, roughness exponents and fractal dimensions were computed. The fractal dimension decreased with increasing substrate temperature and roughness. The surfaces of LiF films were shown to be self-affine
Yadav et al. [13]/2017	The study investigated the fractal properties of ZnO prepared by atom beam sputtering on Si at varying deposition angles- 20°, 30°, 40°, 60°, 75°	Higuchi's algorithm	Fractal dimension and Hurst exponent were determined. The highest fractal dimensions were reported at 30° and 60° while the lowest at 75°. The highest Hurst exponent was determined at 75°. The surfaces were said to be self-affine
Yadav et al. [1]/2012	The fractal and multifractal analysis were performed on electron beam prepared LiF thin film surfaces at different thicknesses (10, 20 and 40 nm)	Autocorrelation, height-height correlation and multifractal detrended fluctuation analysis (MFDFA)	The lateral correlation length and fractal dimensions were seen to increase with film's thickness; whereas the roughness exponent decreased with the thickness of the film
Buchko et al. [40]/2001	The study reports on the fractal analysis of protein polymer films prepared through electrostatic atomization and gas evolution foaming. The films were prepared at different polymer concentration (1.6–2.4 wt%), the electric field (3–6 kV/cm), deposition separation (1–2 cm) and time (1–10 s)	Power spectral density	The fractal dimensions were computed as 2.7 for fibre-only films and 2025 for fiber + bead films. For the bead-only film, the fractal dimension value did not have any physical meaning

(continued)

Table 1 (continued)

Author/year	Description of the publication	Fractal analysis method(s) used	Findings and inferences
Dallaeva et al. [31]/2014	The fractal analyses of AlN epilayers prepared through magnetron sputtering at varying substrate temperatures of 1000, 1300 and 1500 K are reported. The films were deposited on Al_2O_3 substrates	Morphological envelops (cube counting method)	The fractal dimension was computed and shown to increase with a deposition temperature of the substrate
Arman et al. [41]/2015	Fractal analysis of AFM micrographs of Cu films deposited on Si and glass substrates was reported. The films were prepared through DC magnetron sputtering at different thicknesses (5, 25 and 50 nm)	Autocorrelation function, Box (cube) counting and power spectral density methods	The fractal dimensions were computed and were shown to decrease with the increase in the thickness of the film. The results show that sputtered Cu thin films are self-affine and can be characterised through fractal methods
Ţălu et al. [42]/2018	The fractal nature of oxidised CdTe surfaces was investigated using AFM	Autocorrelation, height-height and power spectral density functions	The micromorphology description based on the various fractal techniques was satisfactory to describe the surface oxidation of CdTe
Ţălu et al. [43]/2016	Surface analysis of Cu/Co nanoparticles prepared by DC magnetron sputtering on Si was undertaken under various power and deposition times	Autocorrelation function	Evolution of correlation lengths, pseudo-topothesy and fractal dimensions with various deposition parameters were reported
Tălu et al. [44]/2016	Fractal analysis of gold nanoparticles in carbon film deposited through rf magnetron sputtering was reported. The sputtering was undertaken under varying power (80–120 W)	Autocorrelation and height-height (structural) functions	Fractal dimensions, pseudo-topothesy and corner frequency, were computed as a function of the sputtering power. There were no proportional relationships among fractal dimension, pseudo-topothesy and roughness

(continued)

Table 1 (continued)

Author/year	Description of the publication	Fractal analysis method(s) used	Findings and inferences
Yadav et al. [6]/2015	Fractal and multifractal analysis of BaF_2 thin films deposited on Si by electron beam evaporation. The surfaces of the films were irradiated at different ions/cm^2	Autocorrelation, multifractal and power spectral density functions	Lateral correlation lengths, power spectral density, roughness exponent and fractal dimensions were computed
Hosseinpanahi et al. [45]/2015	The paper reported on the fractal and multifractal analysis of CdTe films deposited on glass substrates by sputtering at varying times of 5, 10 and 15 min and at a constant power of 30 W	Detrended fluctuation analysis (DFA) and MFDFA	Multifractal parameters and Hurst exponent were computed. The Hurst exponent was shown to be higher than 0.5, indicating a positive correlation and multifractal nature of the films
Nasehnejad et al. [46]/2017	Dynamic scaling analysis of electrodeposited silver thin films is reported. The films were prepared at varying thicknesses (80, 150, 220, 320, 600 and 750 nm)	Power spectral density, height-height correlation	Roughness exponent, power spectrum and correlation functions were computed. The power spectral density and correlation functions were seen to increase with the film thickness indicating dynamic scaling of the films. The roughness characteristics were observed to also increase with film's thickness
Raoufi [38]/2009	The fractal analysis of ITO films prepared through electron beam evaporation was undertaken. The analysis was done on as-deposited, annealed samples (200 and 300 °C)	Box-counting method	Fractal dimension was computed for the three AFM micrographs, and higher values were determined on the as-deposited sample. The fractal dimension was shown to decrease with an annealing temperature of the ITO thin films

(continued)

Table 1 (continued)

Author/year	Description of the publication	Fractal analysis method(s) used	Findings and inferences
Raoufi [3]/2010	A power spectral density analysis was reported for electron beam evaporated ITO thin films annealed at various temperatures. The annealing temperatures varied as 0, 250, 350 and 450 °C	Power spectral density function	The fractal dimensions and slope of the inverse power law were computed. The fractal dimension and roughness were seen to increase with annealing temperature whereas the slope decreased with the annealing temperature
Douketis et al. [47]/1995	The fractal characteristics of vacuum-deposited films at 100 and 300 K were investigated	Cube counting, triangulation and power spectrum analyses	For the three methods, fractal dimension was computed and averaged. The highest value of fractal dimension was shown to correspond to films with high roughness
Ţălu et al. [48]/2018	The study investigated the fractal character of ITO deposited by DC magnetron sputtering under different sputtering chamber conditions (O_2, N_2 and H_2 gases)	Autocorrelation function	Fractal dimension and pseudo topothesy were computed and shown to vary with different deposition conditions
Mwema et al. [24]/2018	A power spectral density analysis was undertaken on Al thin films deposited on stainless and mild steel substrates at 150 and 200 W	Power spectral density function	Correlation length, roughness exponent, fractal dimension and Hurst exponent were determined. The fractal characteristics were seen to evolve with the substrate type and rf power
Li et al. [49]/2000	The fractal model was developed to study the self-affine nature of Co-based thin films	Variation-correlation function	The fractal dimension and correlation length were calculated. The fractal dimension was shown to decrease with an increase in surface roughness. The lowest fractal length was reported at the lowest surface roughness

The advantage of these techniques over the statistical techniques of surface analysis of thin films is that they describe the lateral development of the surface features rather than just the vertical features. Through fractal analysis, researchers can deeply understand the growth and scaling of thin films during deposition at various process parameters and techniques. Despite the extensive use of fractal methods, there has been no much efforts to determine the best technique for analysing thin films. Future researches on fractal studies, therefore, should undertake comparative studies of the behaviour of different techniques on the morphological data to determine the suitable algorithm for specific films. There is also increasing application of multifractal analysis for films' surfaces exhibiting multifractal behaviours.

Acknowledgements The authors wish to acknowledge the University Research Committee (URC), University of Johannesburg, South Africa for financing the Ph.D. researcher working on thin film processing.

References

1. Yadav RP, Dwivedi S, Mittal AK, Kumar M, Pandey AC (2012) Fractal and multifractal analysis of LiF thin film surface. Appl Surf Sci 261:547–553
2. Valle F, Brucale M, Chiodini S, Bystrenova E, Albonetti C (2017) Nanoscale morphological analysis of soft matter aggregates with fractal dimension ranging from 1 to 3. Micron 100:60–72
3. Raoufi D (2010) Fractal analyses of ITO thin films: a study based on power spectral density. Phys B Condens Matter 405(1):451–455
4. Barrera E, Gonzalez F, Rodriguez E, Alvarez-Ramirez J (2010) Correlation of optical properties with the fractal microstructure of black molybdenum coatings. Appl Surf Sci 256(6):1756–1763
5. Mandelbrot BB (1985) Self-affine fractals and fractal dimension. Phys Scr 32:257–260
6. Yadav RP, Kumar M, Mittal AK, Pandey AC (2015) Fractal and multifractal characteristics of swift heavy ion induced self-affine nanostructured BaF 2 thin film surfaces. Chaos Interdiscip J Nonlinear Sci 25(8):83115
7. Yehoda JE, Messier R (1985) Are thin film physical structures fractals? Appl Surf Sci 22–23(2):590–595
8. Feng F et al (2018) Surface scaling analysis of textured MgO thin films fabricated by energetic particle self-assisted deposition. Appl Surf Sci 437:287–293
9. Jing C, Tang W (2016) Ga-doped ZnO thin film surface characterization by wavelet and fractal analysis. Appl Surf Sci 364:843–849
10. Kong YL, Muniandy SV, Sulaiman K, Fakir MS (2017) Random fractal surface analysis of disordered organic thin films. Thin Solid Films 623:147–156
11. Dinner O, Paz Y, Grader GS (2018) Orthogonal fractal growth of CsI domains forming a ladder-like structure. Thin Solid Films 661:108–115
12. Yadav RP, Kumar M, Mittal AK, Dwivedi S, Pandey AC (2014) On the scaling law analysis of nanodimensional LiF thin film surfaces. Mater Lett 126:123–125
13. Yadav, RP et al (2017) Effect of angle of deposition on the Fractal properties of ZnO thin film surface. Appl Surf Sci 416:51–58
14. Ţălu S, Stach S, Sueiras V, Ziebarth NM (2015) Fractal analysis of AFM images of the surface of Bowman's membrane of the human cornea. Ann Biomed Eng 43(4):906–916
15. Tokas RB, Jena S, Thakur S, Sahoo NK (2016) Effect of angle of deposition on micro-roughness parameters and optical properties of HfO_2 thin films deposited by reactive electron beam evaporation. Thin Solid Films 609:42–48

16. Senthilkumar M, Sahoo NK, Thakur S, Tokas RB (2005) Characterization of microroughness parameters in gadolinium oxide thin films: a study based on extended power spectral density analyses. Appl Surf Sci 252(5):1608–1619
17. Ţălu S et al (2017) Application of Mie theory and fractal models to determine the optical and surface roughness of Ag–Cu thin films. Opt Quantum Electron 49(7):1–15
18. Wang Y, Xu KW (2004) Characterization of surface morphology of copper tungsten thin film by surface fractal geometry and resistivity. Thin Solid Films 468(1–2):310–315
19. Roy A, Sundaravel B, Batabyal R, Dev BN (2012) Fractal pattern formation in thermal grooving at grain boundaries in Ag films on Si(111) surfaces. Thin Solid Films 520(15):5086–5090
20. Nečas D, Klapetek P (2013) One-dimensional autocorrelation and power spectrum density functions of irregular regions. Ultramicroscopy 124:13–19
21. To, TBT, de Sousa, VB, Aarão Reis, FDA (2018) Thin film growth models with long surface diffusion lengths. Phys A Stat Mech Appl
22. Nečas D, Klapetek P (2012) Gwyddion: an open-source software for SPM data analysis. Cent Eur J Phys 10(1):181–188
23. Carpinteri A, Chiaia B, Invernizzi S (1999) Three-dimensional fractal analysis of concrete fracture at the meso-level. Theor Appl Fract Mech 31(3):163–172
24. Mwema FM, Oladijo OP, Sathiaraj TS, Akinlabi ET (2018) Atomic force microscopy analysis of surface topography of pure thin aluminium films. Mater Res Express 5(4):1–15
25. Starodubtseva MN, Starodubtsev IE, Starodubtsev EG (2017) Novel fractal characteristic of atomic force microscopy images. Micron 96:96–102
26. Klinkenberg B (1994) A review of methods used to determine the fractal dimension of linear features. Math Geol 26(1):23–46
27. Starodubtseva MN, Kuznetsova TG, Chizhik SA, Yegorenkov NI (2007) Atomic force microscopy observation of peroxynitrite-induced erythrocyte cytoskeleton reorganization. Micron 38(8):782–786
28. Annadhason A (2012) Methods of fractal dimension computation. IRACST Int J Comput Sci Inf Technol Secur 2(1):2249–9555
29. Torkhov NA, Bozhkova VG, Ivonin IV, Novikov VA (2009) Determination of the fractal dimension for the epitaxial n-GaAs surface in the local limit. Semiconductors 43(1):33–41
30. Mwema FM, Oladijo OP, Akinlabi ET (2018) Effect of substrate temperature on aluminium thin films prepared by RF-magnetron sputtering. Mater Today Proc. 5(9):20464–20473
31. Dallaeva D, Ţălu S, Stach S, Skarvada P, Tomanek P, Grmela L (2014) AFM imaging and fractal analysis of surface roughness of AlN epilayers on sapphire substrates. Appl Surf Sci 312:81–86
32. Ţălu S, Stach S, Raoufi D, Hosseinpanahi F (2015) Film thickness effect on fractality of tin-doped In_2O_3 thin films. Electron Mater Lett 11(5):749–757
33. Astinchap B (2019) Fractal and statistical characterization of Ti thin films deposited by RF-magnetron sputtering: the effects of deposition time. Optik (Stuttg) 178:231–242
34. Ţălu S et al (2016) Micromorphology and fractal analysis of nickel–carbon composite thin films. J Mater Sci: Mater Electron 27(11):11425–11431
35. Ţălu S et al (2015) Microstructure and tribological properties of FeNPs@a-C: H films by micromorphology analysis and fractal geometry. Ind Eng Chem Res 54(33):8212–8218
36. Dash P et al (2009) Surface roughness and power spectral density study of SHI irradiated ultra-thin gold films. Appl Surf Sci 256(2):558–561
37. Raoufi D, Kiasatpour A, Fallah HR, Rozatian ASH (2007) Surface characterization and microstructure of ITO thin films at different annealing temperatures. Appl Surf Sci 253(23):9085–9090
38. Raoufi D (2009) Morphological characterization of ITO thin films surfaces. Appl Surf Sci 255(6):3682–3686
39. Stach S et al (2017) 3-D surface stereometry studies of sputtered TiN thin films obtained at different substrate temperatures. J Mater Sci: Mater Electron 28(2):2113–2122
40. Buchko CJ, Kozloff KM, Martin DC (2001) Surface characterization of porous, biocompatible protein polymer thin films. Biomaterials 22(11):1289–1300

41. Arman A, Ţălu S, Luna C, Ahmadpourian A, Naseri M, Molamohammadi M (2015) Micromorphology characterization of copper thin films by AFM and fractal analysis. J Mater Sci: Mater Electron 26(12):9630–9639
42. Ţălu S, Pratap R, Sik O, Sobola D, Dallaev R (2018) How topographical surface parameters are correlated with CdTe monocrystal surface oxidation. Mater Sci Semicond Process 85:15–23
43. Ţălu S et al (2016) Microstructure and micromorphology of Cu/Co nanoparticles: surface texture analysis. Electron Mater Lett 12(5):580–588
44. Tălu S et al (2016) Gold nanoparticles embedded in carbon film: micromorphology analysis. J Ind Eng Chem 35:158–166
45. Hosseinpanahi F, Raoufi D, Ranjbarghanei K, Karimi B, Babaei R, Hasani E (2015) Fractal features of CdTe thin films grown by RF magnetron sputtering. Appl Surf Sci 357:1843–1848
46. Nasehnejad M, Nabiyouni G, Shahraki MG (2017) Dynamic scaling study of nanostructured silver films. J Phys D Appl Phys 50(37)
47. Douketis C, Wang Z, Haslett ZL, Moskovits M (1995) Fractal character of cold-deposited silver films determined by low-temperature scanning tunneling microscopy. Phys Rev B: Condens Matter 51(16):11022–11031
48. Ţălu S et al (2018) Micromorphology analysis of sputtered indium tin oxide fabricated with variable ambient combinations. Mater Lett 220:169–171
49. Li JM, Lu L, Su Y, Lai MO (2000) Self-affine nature of thin film surface. Appl Surf Sci 161(1):187–193